Caveolae from luminal plasmalemma of rat lung endothelium: Microdomains enriched in caveolin, Ca²⁺-ATPase, and inositol trisphosphate receptor

JAN E. SCHNITZER*†, PHIL OH*, B. S. JACOBSON‡, AND ANN M. DVORAK*

*Department of Pathology, Harvard Medical School, Beth Israel Hospital, 99 Brookline Avenue, Boston, MA 02215; and ‡Department of Biochemistry, University of Massachusetts, Amherst, MA 01003

ABSTRACT A distinctive feature of many endothelia is an abundant population of noncoated plasmalemmal vesicles, or caveolae. Caveolae have been implicated in many important cellular processes, including transcytosis, endocytosis, potocytosis, and even signal transduction. Because caveolae have not been purified from endothelial cell surfaces, little is known directly about their structure and function in the endothelium. To delineate the transport role of these caveolae, we purified them from isolated luminal endothelial plasma membranes of rat lung. The rat lung luminal endothelial cell surfaces were isolated after coating them, *in situ*, with positively charged colloidal silica. The caveolae were then separated from these coated membranes and purified to yield a homogeneous population of morphologically distinct vesicles enriched in the structural protein caveolin. As with caveolae found on the endothelial cell surface *in vivo*, these highly purified caveolae contained the plasmalemmal Ca²⁺-ATPase and inositol 1,4,5-trisphosphate surface receptors. By contrast, other plasma membrane proteins were excluded from the caveolae, including angiotensin-converting enzyme, β-actin, and band 4.1. The purified caveolae appeared to represent specific microdomains of the cell surface with their own unique molecular topography.

Vesicular transport plays a fundamental role in many cellular functions. The importance of clathrin-coated vesicles in receptor-mediated endocytosis and transcytosis has been established at least in part as a result of their purification. Molecules binding to the cell surface can also be internalized by clathrin-independent pathways, sometimes via clustering within noncoated vesicles (1, 2). Non-clathrin-coated vesicles of about 70–100 nm in diameter, known as caveolae, are thought to contribute significantly to endocytosis and transcytosis, especially in endothelium (for review, see ref. 3). In most organs, the endothelium is the critical barrier preventing the passage of molecules and cells from the circulating blood to the underlying tissue cells. Specific proteins have been identified on the endothelial cell surface that mediate selective transport of important blood proteins, apparently via the abundant population of caveolae found in certain endothelia (3–5). In agreement with a role for caveolae in transport, recent studies have shown that agents that disassemble endothelial caveolae reduce the endocytosis, transcytosis, and transcapillary permeability of select macromolecules (2). Caveolae have been implicated in other important cellular functions, including potocytosis (6) and signal transduction (7–9). Caveolar functions probably vary according to cell type. Morphological differences have been noted *in situ* for caveolae found in endothelium versus epithelium (10).

Three proteins originally discovered in other cell types have been found *in situ* by immunoelectron microscopy to be ex-

pressed on the surface of endothelium, concentrated in caveolae: the plasmalemmal Ca²⁺-ATPase (9), inositol 1,4,5-trisphosphate (IP₃) receptor (8), and caveolin (also called VIP-21) (11–13). Much of the uncertainty about caveolar function stems from the paucity of information available at the molecular level. One contributing factor to this lack of knowledge is that these cell surface organelles have not been purified to homogeneity from endothelium. Here, we describe a strategy for purifying caveolae *in situ* from the endothelium in the rat lung. First, the luminal endothelial plasmalemma with its subtending caveolae was selectively isolated from the rat lung microvasculature. Then, the caveolae were purified from this plasmalemmal fraction in order to begin their biochemical dissection into structural and functional components.

METHODS

Antibodies. Mouse monoclonal antibody to caveolin was from Zymed or Transduction Laboratories (Lexington, KY); rabbit polyclonal antibody to angiotensin converting enzyme (ACE) was from R. Skidgel (University of Illinois); rabbit polyclonal antibody to band 4.1, from V. Marchesi (Yale University); mouse monoclonal antibody to Ca²⁺-ATPase, from Affinity BioReagents (Neshanic Station, NJ); mouse monoclonal antibody to β-actin, from Sigma; and goat polyclonal antibody to IP₃ receptor, from Solomon H. Snyder and Alan Sharp (Johns Hopkins University). Sources for other reagents were as before (2, 4, 5, 14).

In Situ **Perfusion of Rat Lungs for Silica Coating of the Luminal Endothelial Cell Surface.** The lungs of anesthetized male Sprague–Dawley rats were ventilated after tracheotomy and then perfused as described (5, 14). In brief, the right cardiac ventricle was injected with 0.5 ml of Ringer's solution at pH 7.4 (111 mM NaCl/2.4 mM KCl/1 mM MgSO₄/5.5 mM glucose/5 mM Hepes/0.195 mM NaHCO₃) containing 30 μM nitroprusside and 175 units of heparin before cannulation of the pulmonary artery. The lungs were perfused at 8–10 mmHg (1 mmHg = 133 Pa) with the following solutions (all at 10–12°C except as noted) in order: (*i*) oxygenated Ringer's solution containing 30 μM nitroprusside for 90 sec at room temperature and then for 3.5 min at 10–12°C; (*ii*) MBS (125 mM NaCl/20 mM Mes, pH 6.0) for 90 sec; (*iii*) 1% colloidal silica in MBS; (*iv*) MBS for 90 sec, to clear free silica from vasculature; (*v*) 1% sodium polyacrylate in MBS for 90 sec, to crosslink and shield membrane-bound silica; and (*vi*) 8–10 ml of Hepes-buffered sucrose with protease inhibitors [HBS+, pH 7, contains 0.25 M sucrose, 25 mM Hepes, leupeptin (10 μg/ml), pepstatin A (10 μg/ml), o-phenanthroline (10 μg/ml), 4-(2-aminoethyl)benzenesulfonyl fluoride (10 μg/ml), and *trans*-epoxysuccinyl-L-leucinamido(4-guanidino)butane (50 μg/ml)]. The lungs were excised and immersed in cold HBS+.

Purification of Luminal Endothelial Cell Membranes. The chilled rat lungs were weighed, minced with a razor blade in a plastic dish on an aluminum block embedded in crushed ice, and then added to 20 ml of cold HBS+ for homogenization (12 strokes) in a type C Teflon pestle/glass homogenizer with a high-speed motor run at 1800 rpm. After filtration through a 0.53-μm Nytex net followed by a 0.3-μm net, the homogenate was mixed with 102% (wt/vol) Nycodenz (Accurate Chemical and Scientific) with 20 mM KCl to make a 50% final solution and was layered over a 55–70% Nycodenz continuous gradient containing 20 mM KCl plus HBS. After centrifugation in a Beckman SW28 rotor at 15,000 rpm for 30 min at 4°C, the pellet was suspended in 1 ml of MBS and named P.

Purification of Caveolae from Silica-Coated Endothelial Cell Membranes. Cold 10% (vol/vol) Triton X-100 was added to the suspended membrane pellet (P) as described above to make a final concentration of 1%. After nutation for 10 min at 4°C, the suspension was homogenized in a type AA Teflon pestle/glass homogenizer (10 strokes) and then brought to 40% sucrose and 20 mM KCl. A 35–0% sucrose gradient in 20 mM KCl was layered over the homogenate in a Beckman SW55 rotor tube and then centrifuged at 4°C overnight at 30,000 rpm. A membrane layer clearly visible between 10% and 16% sucrose was collected, labeled V, and then diluted 3-fold with MBS before centrifugation for 2 hr at 13,000 × g at 4°C. The resultant pellet was either processed for electron microscopy or SDS/PAGE. In attempting to optimize the conditions for isolation of caveolae, we found that the low-density caveolar fraction was not altered by (*i*) the presence of Triton X-100 throughout the sucrose gradient during centrifugation and (*ii*) the absence of Triton X-100 during homogenization, except that the yield of caveolae was diminished. Triton X-100 appears to facilitate the shearing of the caveolae away from the plasma membrane.

ELISA. After the sucrose density centrifugation described above, 33 fractions of 150 μl were collected and the pellet was suspended in 150 μl of MBS (fraction 34). Aliquots of each fraction (50–100 μl) were placed in individual wells of a 96-well tray for drying overnight. After washing, the wells were blocked for 1 hr with ELISA wash buffer (EWB: 2% ovalbumin/2 mM CaCl$_2$/164 M NaCl/57 mM phosphate, pH 7.4), incubated for 1 hr with EWB containing antibodies (1:200) to either caveolin or ACE, washed for 1 min in EWB three times, incubated with reporter antibody conjugated to horseradish peroxidase (1:500 in EWB), and washed again. Substrate solution (50 mM Na$_2$HPO$_4$/25 mM citric acid/0.12% o-phenylenediamine dihydrochloride/0.03% H$_2$O$_2$) was added and the reaction was stopped with 4 M H$_2$SO$_4$ before the signal was read with a Molecular Devices Thermomax microplate reader.

SDS/PAGE and Immunoblotting. As reported (5, 14), the proteins of various tissue fractions were solubilized and separated by SDS/PAGE in 5–15% gels for direct analysis by silver staining or electrotransfer to nitrocellulose or poly(vinylidene difluoride) (Immobilon; Millipore) filters for immunoblotting using primary antibodies followed by appropriate ^{125}I-labeled reporter antibodies. Band intensities were quantified by PhosphorImager (Molecular Dynamics), densitometry of autoradiograms, and/or direct counting of γ radioactivity. Protein assays were performed with the Bio-Rad BCA kit.

RESULTS

Isolation of caveolae associated with the endothelial cell surface has many difficulties. The endothelium represents but a small percentage of a diverse population of cells in any organ. Unfortunately, isolating endothelial cells from tissues as a primary source or even for growth in culture causes morphological changes, including a very significant loss in cell surface caveolae (15). Also, noncoated vesicles that are very similar in size and density to plasmalemmal caveolae and may even contain the caveolar marker protein caveolin (11, 12) may be found in other cellular compartments such as the trans-Golgi network. Moreover, caveolae may vary according to cell type (10). To overcome the above problems, we utilized a strategy of first isolating in high yield and purity the luminal endothelial plasma membranes with associated caveolae from rat lungs *in situ*. The caveolae were then removed and isolated from this membrane fraction (Fig. 1).

Purification of Luminal Endothelial Cell Membranes from Rat Lungs Perfused *in Situ*. The rat lung microvasculature was perfused via the pulmonary artery with a positively charged colloidal silica solution to coat the luminal endothelial cell membrane normally exposed to the circulating blood and create a stable adherent silica pellicle that marks this specific membrane of interest (14). Such a coating increased the membrane's density and was so strongly attached to the plasma membrane that after tissue homogenization, large sheets of silica-coated membrane with attached caveolae were readily isolated away from other cellular membranes and debris by centrifugation through a high-density medium (14). The silica-coated membranes displayed ample enrichment for endothelial cell surface markers and little contamination from other tissue components. As shown in our past work (14) and in Fig. 2, the typical isolated membrane sheet had caveolae attached on one side and a silica coating on the other side. By SDS/PAGE, the silica-coated membranes had a protein profile quite distinct from that of the starting lung homogenate (Fig. 3). Moreover, quantitative immunoblotting (Fig. 3 and Table 1) revealed enrichments up to 30-fold in the silica-coated membrane pellets relative to the starting tissue homoge-
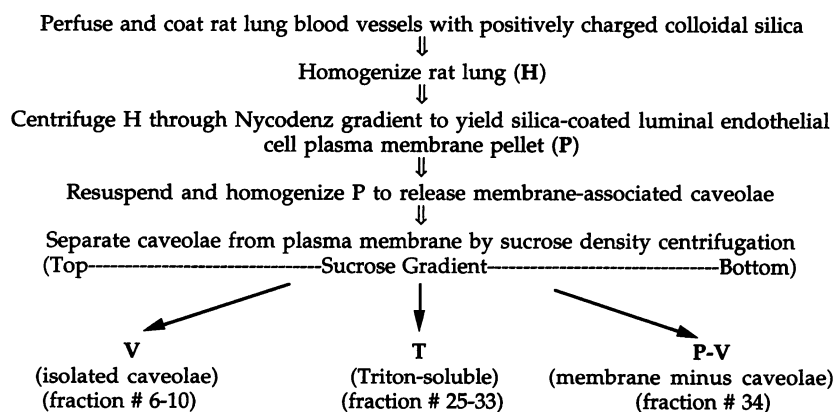
Perfuse and coat rat lung blood vessels with positively charged colloidal silica
⇓
Homogenize rat lung (H)
⇓
Centrifuge H through Nycodenz gradient to yield silica-coated luminal endothelial
cell plasma membrane pellet (P)
⇓
Resuspend and homogenize P to release membrane-associated caveolae
⇓
Separate caveolae from plasma membrane by sucrose density centrifugation
(Top--------------------------------Sucrose Gradient--------------------------------Bottom)

V	T	P-V
(isolated caveolae)	(Triton-soluble)	(membrane minus caveolae)
(fraction # 6-10)	(fraction # 25-33)	(fraction # 34)

Fig. 1.   Procedure for purification of endothelial caveolae.

Cell Biology: Schnitzer *et al.*

Proc. Natl. Acad. Sci. USA 92 (1995)   1761

nate for several proteins known to be expressed on the surface of endothelium, such as caveolin (11) and ACE (16). Conversely, proteins of intracellular organelles (cytochrome oxidase and ribophorin) and even the plasma membranes of other lung tissue cells (fibroblast surface antigen) were excluded from this membrane fraction.

Detergent Resistance of Caveolin as a Marker for Caveolae. We used caveolin as a biochemical marker for caveolae and found that the caveolin abundantly expressed in the silica-coated membranes was resistant to solubilization by homogenization at 4–8°C using Triton X-100 (Fig. 3) or 3-[(3-cholamidopropyl)dimethylammonio]-1-propanesulfonate but not other detergents, including octyl β-D-glucoside, SDS, deoxycholate, and Nonidet P-40 (data not shown). SDS/PAGE revealed that many proteins in silica-coated membranes were solubilized by Triton X-100, whereas others were not and could be sedimented by centrifugation. Immunoblotting showed that caveolin and the cytoskeletal protein band 4.1 were sedimented into the Triton-insoluble fraction, whereas ACE was found primarily in the Triton-soluble fraction.

Isolation of Vesicles Stripped from Silica-Coated Membranes. The silica-coated membranes (P) in Triton X-100 were stripped of protruding caveolae by shearing in a homogenizer and then subjected to sucrose density centrifugation to isolate the caveolae (see *Methods* and Fig. 1). Analysis of 34 fractions from the sucrose gradient revealed a peak signal for caveolin well separated from that for ACE (Fig. 4). Little caveolin was detected in the silica-coated membrane after removal of the vesicles (P−V). Most of it was in the visible membrane band at 10–16% sucrose (fractions 6–10), which was collected,

labeled V for vesicles, and examined by electron microscopy, SDS/PAGE, and immunoblotting.

Characterization of Isolated Vesicles as Caveolae. As shown in Fig. 2, electron microscopy was performed (as in ref. 17) on the three main membrane fractions: original silica-coated membrane (P), isolated vesicles (V), and the silica-coated membrane pellet after removal of vesicles (P−V). In P, small, membrane-bound, electron-lucent openings, or fenestrae, were visible in many vesicles in favorable sections (arrow, Fig. 2B) and clearly were not part of the ostia of the caveolae directly at the cell membrane surface. These fenestrae, as described many years ago (18), are characteristic of endothelial caveolae and probably indicate a previous attachment to another vesicle as part of a chain of vesicles. The P−V fraction contained silica-coated membranes without attached caveolae (Fig. 2C). The V fraction contained a rather uniform distribution of small noncoated vesicles, primarily with diameters of 50–100 nm (Fig. 2D). Higher magnification revealed vesicular structures typical for caveolae *in vivo* (Fig. 2 E–G). Single plasmalemmal vesicles and chains of membrane-bound vesicles were present. The fenestrae distinctive for caveolae were easily visible in many of the vesicles (arrow, Fig. 2E). Some vesicles still maintained their narrowed necks (arrowhead, Fig. 2E) as in caveolae that are attached to the plasmalemma of endothelium *in vivo*. Higher magnification showed central, membrane-bound fenestrae within the isolated caveolae (Fig. 2 F and G). Central dense, rounded knobs as described originally *in vivo* (18) could be found within some of these fenestrae (unpublished observations).

Biochemical analysis revealed a distinct protein profile for the isolated vesicles, with not only very evident enrichment of
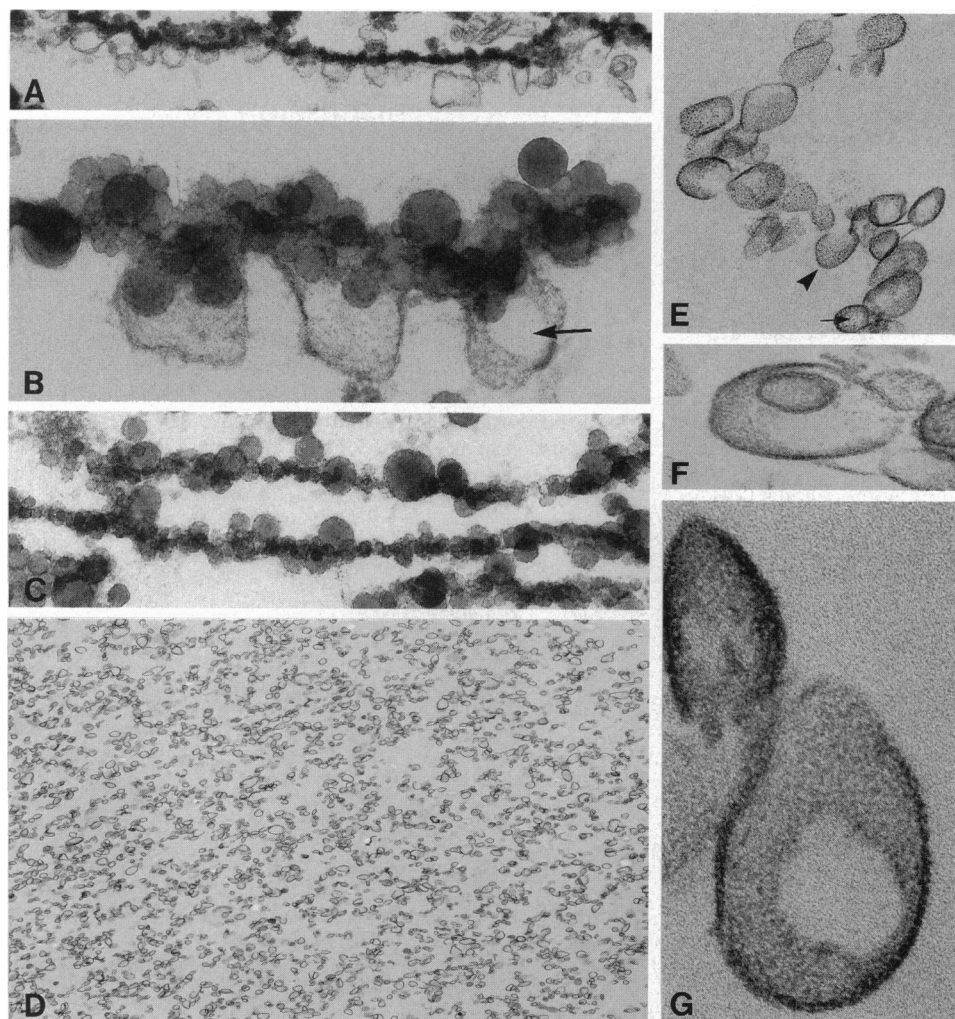

FIG. 2. Electron microscopy of the silica-coated luminal endothelial plasma membrane and derived caveolae. Fractions processed for electron microscopy included P, V, and P−V (see Fig. 1). (*A*) P fraction, showing electron-dense silica particles bound to plasma membrane with at least 15 caveolae attached. (×24,500.) (*B*) P fraction, showing silica-coated membrane with 3 caveolae attached. Note their trilaminar unit membranes; one shows an electron-lucent opening, or fenestra (arrow). (×88,200.) (*C*) P−V fraction. Silica-coated plasma membranes do not have caveolae attached. (×64,400.) (*D*) V fraction. Low-magnification view shows a homogeneous collection of small vesicles. (×5950.) (*E*) V fraction. Purified caveolae, arranged in clusters and chains, show focal electron-lucent fenestrae (arrow). One vesicle (arrowhead) is attached to a narrowed neck, exactly like that seen *in vivo*, where vesicles attach to luminal plasma membranes. (×59,500.) (*F*) V fraction. A trilaminar unit membrane-bound plasmalemmal vesicle has a trilaminar unit-bound fenestra. (×82,600.) (*G*) V fraction. This cross-sectional, high-magnification view shows that the trilaminar unit membrane nearly encloses this vesicle. The apical (luminal) portion of this tear drop-shaped structure appears open. The contents of the vesicle are slightly electron-dense, and centrally located is an electron-lucent, membrane-bound fenestra. (×203,000.)
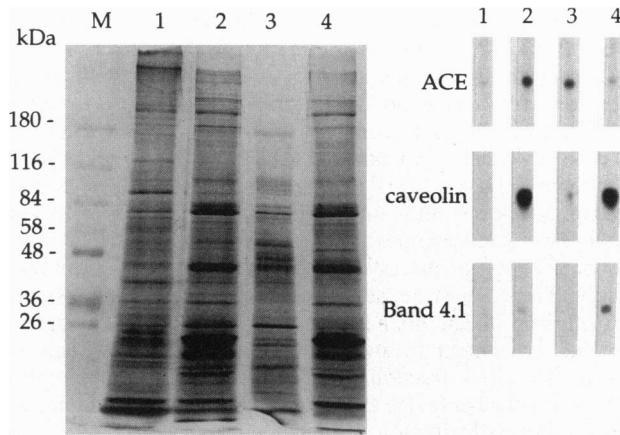
FIG. 3.   Extraction of proteins from the purified endothelial cell membranes with Triton X-100. (*Left*) Silver stain of SDS/PAGE analysis of proteins (5 μg per lane) from various rat lung fractions. Whole rat lung homogenate (lane 1) was sedimented as described in *Methods* to yield the silica-coated membrane pellet (lane 2). This membrane pellet was suspended at 4°C in 1% Triton X-100, homogenized, and centrifuged at 13,000 × g for 1 hr. The solubilized and sedimented proteins are shown in lanes 3 and 4, respectively. Lane M, size markers. (*Right*) Representative immunoblots for test proteins (ACE, caveolin, and band 4.1) found in the equivalent fractions listed in *A*.
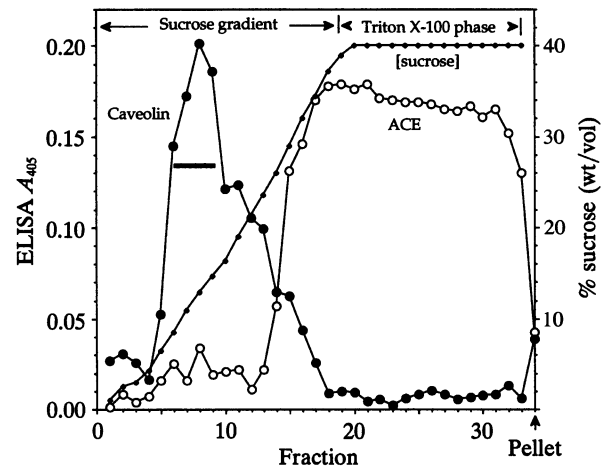

FIG. 4.   Fraction analysis of sucrose density gradient of silica-coated endothelial cell membranes treated to release caveolae. Fractions collected from the top after sucrose density centrifugation of the Triton X-100 homogenates were used in ELISA with antibodies specific for the indicated proteins. Protein assay of the fractions in the sucrose gradient also showed a peak at fraction 9. The heavy bar in the caveolin peak indicates the fractions collected and labeled V.

various proteins relative to the starting membrane pellet but also exclusion of other proteins (Fig. 5). Immunoblotting showed a significant enrichment in V for caveolin, plasmalemmal Ca^{2+}-ATPase, and IP_3 receptor, with up to a 13-fold enrichment for caveolin and IP_3 receptor relative to original membrane (Table 1). Furthermore, little signal for these proteins remained behind in the silica-coated membrane (P−V) after the caveolae were removed. Immunoblots that were quantified revealed that these three integral membrane proteins were resistant to Triton solubilization and concentrated within the purified caveolae (Fig. 6). Eighty to 95% of the signal for the Ca^{2+} pump, IP_3 receptor, and caveolin was within the caveolar fraction. By contrast, band 4.1 and ACE were excluded. These purified caveolae represented a microdomain of the plasma membrane with at least three resident proteins that were not just freely distributed over the whole cell surface but preferentially localized to this organelle.

The extent of purification of caveolae is indicated by the relative enrichments for caveolin (Table 1). As far as yields, it was previously shown that >90% of the microvasculature *in situ* was coated with silica and at least 80% of the silica-coated membrane was pelleted from the rat lung homogenates (14). The recovery of caveolin in the membrane pellet (P) was 10% of the total detected in the starting homogenate, which was

consistent with the concept that only the plasmalemmal subset of caveolin-containing vesicles from the luminal side of the endothelium was isolated. The yield of plasmalemmal caveolae derived directly from the original silica-coated membranes (P) ranged from 53% to 60% over four separate experiments as indicated by ELISA and immunoblotting for caveolin. Overall, we isolated about 5 μg of total protein which represented about 5–6% of the caveolae in the starting lung homogenates.

DISCUSSION

Various laboratories (7, 11–13, 19–23) have shown that membrane fractions that are resistant to extraction with nonionic detergents can be isolated from tissues and nonendothelial cells (fibroblasts, Madin–Darby canine kidney cells, and smooth muscle cells). They generally isolated intact membrane sheets and to varying degrees a heterogeneous vesicular population which includes small vesicles in some cases shown to contain caveolin (7, 22, 23). Many of these reports noted the presence or enrichment of molecules such as glycosylphosphatidylinositol (GPI)-anchored proteins (7, 19–22) and, surprisingly, the cytoskeletal protein actin (22, 23). We also find ample enrichment for caveolin in our purified caveolar preparation (V), but as quantified in Fig. 6, β-actin is nearly absent.
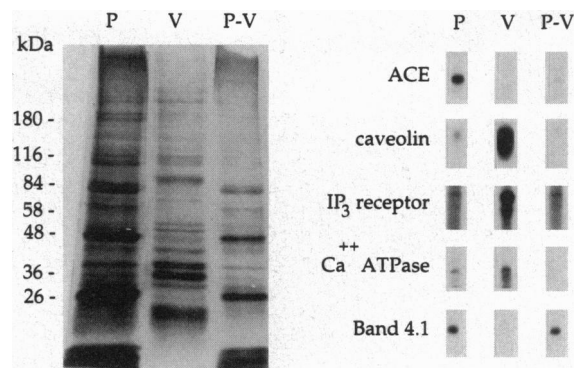
Table 1.   Relative distribution of various proteins in rat lung fractions

Antigen	Pellet/homogenate	Vesicle/pellet
ACE	15	0.08
Caveolin	30	13
Fibroblast surface antigen	0	−
Ca^{2+}-ATPase	8	3
IP_3 receptor	3	12
Band 4.1	15	0.09
Cytochrome oxidase	0	−
Ribophorin	0	−

Data represent a composite of new experiments/antigens and previously reported results (14). Quantified band intensities of immunoblots were normalized per unit of protein before computation of ratios as an average of at least two determinations. The value 0 indicates antigen not detected in P but found in H; − indicates not done.

FIG. 5.   Biochemical characterization of endothelial cell membrane fractions and caveolae isolated *in situ* from rat lung. (*Left*) SDS/PAGE analysis of proteins found in P, V, and P−V. (*Right*) Immunoblots of P, V, and P−V with antibodies specific for the indicated proteins. Protein loads were 5 μg for P and P−V and 2 μg for V.

Cell Biology: Schnitzer *et al.*
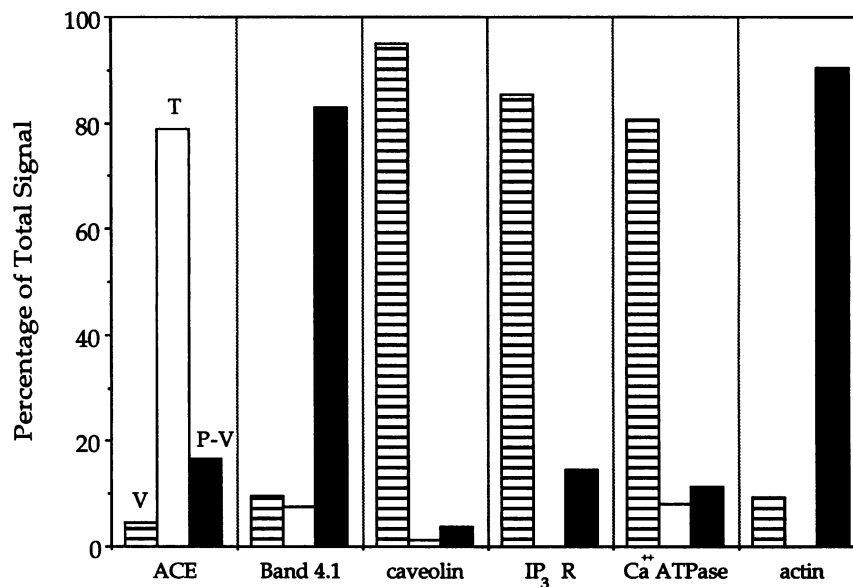
Proc. Natl. Acad. Sci. USA 92 (1995)   1763

FIG. 6. Percent distribution of specific proteins in plasma membrane subfractions. Immunoblots were used to quantify the distribution of the indicated endothelial cell membrane proteins in the three main subfractions of the purified silica-coated membranes after homogenization: V, P−V, and the Triton X-100 soluble fraction (T). Band intensities derived from at least two experiments were normalized per protein loaded and are expressed as the mean percentage of the signal totaled for the three fractions.

Our preliminary data indicate that although the GPI-linked protein 5′-nucleotidase is amply represented in the silica-coated membrane fraction (P), it is actually excluded from the caveolae (V). Because GPI-linked proteins are preferentially found with special membrane lipids that associate into microdomains that exclude detergent (20), this finding could simply be attributed to differential selective solubilization of such microdomains by the Triton X-100. This possibility seems unlikely because 5′-nucleotidase is not extracted by Triton X-100 but remains with the sheared silica-coated membrane devoid of caveolae (P−V). The silica particles are large enough that they are rarely associated with or inside the caveolae (14) yet may be interacting with the GPI-linked proteins found in a microdomain outside of the caveolae (unpublished work).

It appears that by starting in our preparation with a highly purified luminal plasmalemmal fraction of the endothelium in the rat lung, we have (*i*) avoided potential interference of other contaminating membranes in the tissue, including those thought also to contain caveolin—i.e., the Golgi network and trans-Golgi vesicles (11, 12)—and (*ii*) purified a homogeneous population of vesicles that contain little, if any, contamination of other membranes, including possibly other detergent-resistant plasmalemmal microdomains. With this approach for isolating caveolae, the structure and function of this important endothelial cell surface organelle can now be examined in detail with greater confidence at the molecular level.

1. Montesano, R., Roth, J., Robert, A. & Orci, L. (1982) *Nature (London)* **296,** 651–653.

2. Schnitzer, J. E., Oh, P., Pinney, E. & Allard, J. (1994) *J. Cell Biol.* **127,** 1217–1232.
3. Schnitzer, J. E. (1993) *Trends Cardiovasc. Med.* **3,** 124–130.
4. Schnitzer, J. E. & Bravo, J. (1993) *J. Biol. Chem.* **268,** 7562–7570.
5. Schnitzer, J. E. & Oh, P. (1994) *J. Biol. Chem.* **269,** 6072–6082.
6. Anderson, R. G. W., Kamen, B. A., Rothberg, K. G. & Lacey, S. W. (1992) *Science* **255,** 410–411.
7. Sargiacomo, M., Sudol, M., Tang, Z. & Lisanti, M. P. (1993) *J. Cell Biol.* **122,** 789–807.
8. Fujimoto, T., Nakade, S., Miyawaki, A., Mikoshiba, K. & Ogawa, K. (1992) *J. Cell Biol.* **119,** 1507–1513.
9. Fujimoto, T. (1993) *J. Cell Biol.* **120,** 1147–1157.
10. Izumi, T., Shibata, Y. & Yamamoto, T. (1989) *J. Electron Microsc.* **38,** 47–53.
11. Dupree, P., Parton, R. G., Raposo, G., Kurchalia, T. V. & Simons, K. (1993) *EMBO J.* **12,** 1597–1605.
12. Kurzchalia, T. V., Dupree, P., Parton, R. G., Kellner, R., Virta, H., Lehnert, M. & Simons, K. (1992) *J. Cell Biol.* **118,** 1003–1014.
13. Rothberg, K. G., Heuser, J. E., Donzell, W. C., Ying, Y.-S., Glenney, J. R. & Anderson, R. G. W. (1992) *Cell* **68,** 673–682.
14. Jacobson, B. S., Schnitzer, J. E., McCaffery, M. & Palade, G. E. (1992) *Eur. J. Cell Biol.* **58,** 296–306.
15. Schnitzer, J. E., Siflinger-Birnboim, A., Del Vecchio, P. J. & Malik, A. B. (1994) *Biochem. Biophys. Res. Commun.* **199,** 11–19.
16. Caldwell, P. R. B., Seegal, B. C. & Hsu, K. C. (1976) *Science* **191,** 1050–1051.
17. Dvorak, A. M. (1987) *J. Electron Microsc. Tech.* **6,** 255–301.
18. Palade, G. E. & Bruns, R. R. (1968) *J. Cell Biol.* **37,** 633–649.
19. Hoessli, D. & Rungger-Brandle, E. (1985) *Exp. Cell Res.* **156,** 239–250.
20. Hooper, N. M. & Turner, A. J. (1988) *Biochem. J.* **250,** 865–869.
21. Brown, D. & Rose, J. K. (1993) *Cell* **68,** 533–544.
22. Chang, W.-J., Ying, Y., Rothberg, K. G., Hooper, N. M., Turner, A. J., Gambliel, H. A., De Gunzburg, J., Mumby, S. M., Gilman, A. G. & Anderson, R. G. W. (1994) *J. Cell Biol.* **126,** 127–138.
23. Lisanti, M. P., Scherer, P. E., Vidugiriene, J., Tang, Z., Hermanowski-Vosatka, A., Tu, Y. & Sargiacomo, M. (1994) *J. Cell Biol.* **126,** 111–126.